

## ANALYSIS OF STRAIN LOCALIZATION WITH A NONLOCAL PLASTICITY MODEL

MIGUEL A. MÁNICA\*, ANTONIO GENS†, JEAN VAUNAT† AND  
DANIEL F. RUIZ†

\*†Department of Geotechnical Engineering and Geo-sciences  
Universitat Politècnica de Catalunya (UPC)  
Campus Nord, 08034 Barcelona, Spain  
\*e-mail: miguel.angel.manica@estudiant.upc.edu

**Key words:** Strain localization, nonlocal plasticity, plane strain, stiff fine-grained soils

**Abstract.** In the present paper a nonlocal plasticity model is described, intended to reproduce the mechanical behaviour of stiff fine-grained soils, including the objective simulation of strain localization; the phenomenon of accumulation of deformations in narrow zones in the form of shear bands or fractures. A number of analyses have been performed to assess the developed formulation. Relevant aspects have been addressed such as the thickness of the shear band, its orientation, and the onset of localization in a boundary value problem (BVP). Results provide useful insights into relevant aspects of the numerical simulation of strain localization.

### 1 INTRODUCTION

In conventional geotechnical engineering situations stiff fine-grained materials show a quasi-brittle behaviour under deviatoric loading [1]. The resulting strain field is generally non homogeneous and deformations tend to localize into thin zones of intense shearing in the form of fractures or slip surfaces. This phenomenon is known as *strain localization*, observed also in other geomaterials like concrete, rocks or dense sands. The numerical simulation of such phenomenon under the framework of continuum mechanics involves a number of difficulties, as standard formulations tend to deliver non-objective results due to the loss of ellipticity of the governing equation at the onset of localization. This non-objectivity is recognized by a strong dependency of results with the employed mesh; a vanishing energy dissipation and localization into a zone of vanishing volume are obtained by reducing the size of elements. Enriched continuum formulations must be employed, providing the material with an internal length scale, not present in the standard formulation, which tend to prevent the common pathologies arising from the simulation of strain localization.

In this contribution, a nonlocal plasticity model is described, capable of simulating strain localization objectively, without resulting in mesh-dependent results. The model

is intended for the simulation of stiff fine-grained soils. A number of analyses have been performed to assess the developed formulation for the simulation of localized deformation patterns. Relevant aspects have been addressed, such as the thickness of the shear band, its orientation, and the onset of localization in a BVP.

## 2 MODEL FORMULATION

### 2.1 Local model

The local model refers to the employed standard elasto-plastic constitutive law, without the enrichment provided by the nonlocal approach. It is based on the simple conceptual scheme depicted in Fig. 1, for the strength of stiff clays under shearing, where the following characteristic pattern is modelled: after reaching the peak, a first rapid reduction of strength is identified, associated with the degradation and breakage of interparticle bonds; then, a more gentle strength reduction is observed, associated with the realignment of clay particles tending towards the residual state, where no further strength reduction occurs. Experimental evidence supporting this conceptual scheme is summarized in [1], as well as a comprehensive review on the hydromechanical behaviour of these materials.

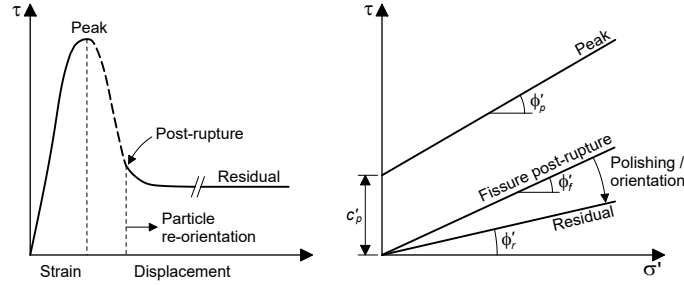


**Figure 1:** Conceptual scheme for the strength of stiff plastic clays [2]

Inside the yield surface, the response is assumed linear elastic. The employed yield criterion is defined by a hyperbolic approximation of the Mohr-Coulomb envelope, expressed as,

$$F = -(c^* + p \tan \phi^*) + \sqrt{\frac{J_2}{f(\theta)} + (c^* + p_t \tan \phi^*)^2} \quad (1)$$

where  $c^*$  is the apparent cohesion,  $\phi^*$  is the apparent friction angle,  $p_t$  is the isotropic tensile strength,  $p$  is the mean stress,  $J_2$  is the second invariant of the deviatoric stress tensor,  $\theta$  is the Lode's angle, and  $f(\theta)$  is a function defining the shape in the octahedral plane. Eq. (1) describes a curved envelope at low mean stresses, with a limited tensile strength, as generally occurs in stiff clayey materials. For high mean stresses, the criterion tends to converge to a linear Mohr-Coulomb envelope, with  $\phi = \phi^*$  and  $c = c^*$ .

Isotropic non-linear hardening/softening was considered in such a way that the main characteristics of the conceptual scheme for the strength of stiff clays (Fig. 1) were incor-

porated. Hardening/softening is driven by the evolution of the strength parameters with plastic strains, characterized by a scalar state variable defined as,

$$\epsilon_{eq}^p = (\boldsymbol{\epsilon}^p : \boldsymbol{\epsilon}^p)^{1/2} \quad (2)$$

where  $\boldsymbol{\epsilon}^p$  is the plastic strain tensor. Strength parameters vary in a piecewise manner as shown in Fig. 2.

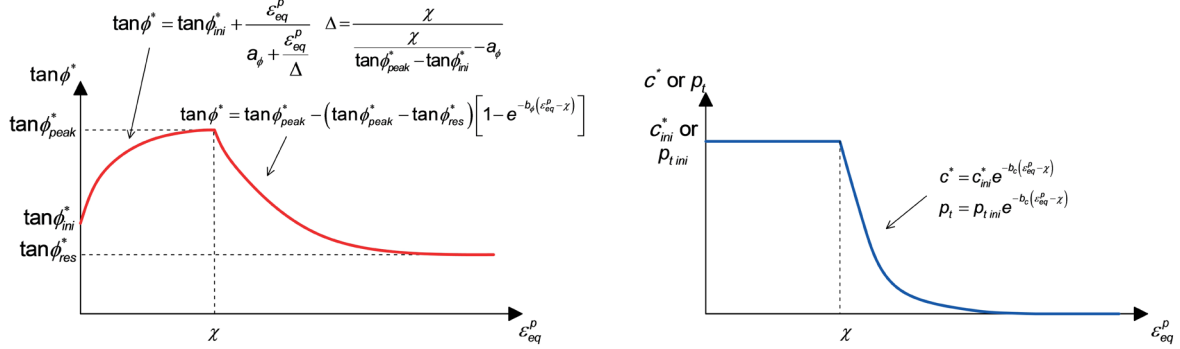


**Figure 2:** Hardening/softening rules

A non-associated flow rule is adopted. Rather than deriving a specific function for the plastic potential, the flow rule is directly obtained in the following way,

$$\frac{\partial G}{\partial \boldsymbol{\sigma}} = \omega \frac{\partial F}{\partial p} \frac{\partial p}{\partial \boldsymbol{\sigma}} + \frac{\partial F}{\partial J_2} \frac{\partial J_2}{\partial \boldsymbol{\sigma}} + \frac{\partial F}{\partial \theta} \frac{\partial \theta}{\partial \boldsymbol{\sigma}} \quad (3)$$

where  $G$  is the plastic potential and  $\omega$  is a constant that controls the volumetric component of plastic deformations.

Other important features exhibited by these materials are not included here, such as stiffness and strength anisotropy, consolidation processes (i.e. hydromechanical coupling), creep, or yielding under volumetric loading. The main purpose of the present work is the objective simulation of localization under deviatoric loading, and therefore the incorporation of these features within the present approach will be addressed in future work.

## 2.2 Nonlocal extension

A nonlocal model is one where the behaviour at a material point (or at a Gauss point in a finite element simulation) depends not only on its state, but also on the state of neighbouring points within a certain region. This is accomplished by replacing a given variable by its nonlocal counterpart. If  $f(\boldsymbol{x})$  is some local field within a body of volume  $V$ , the nonlocal field can be expressed as,

$$\bar{f}(\boldsymbol{x}) = \int_V w(\boldsymbol{x}, \boldsymbol{\xi}) f(\boldsymbol{\xi}) d\boldsymbol{\xi} \quad (4)$$

where  $w(\boldsymbol{x}, \boldsymbol{\xi})$  is a weight function controlling the importance of neighbouring points as a function of its position ( $\boldsymbol{\xi}$ ), relative to the position of the actual point ( $\boldsymbol{x}$ ). Typically,

only the distance between them is considered, and a Gaussian function is employed as the weighting function, where the width of the bell-shaped curve implicitly introduces a length scale to the continuum formulation.

Different nonlocal models are obtained depending on which variable (or variables) is considered nonlocal (see [3] for a comprehensive review). Here, we applied the approach given by [4], for the enrichment of the local model described in Section 2.1. The variable assumed nonlocal is the state variable controlling softening (Eq. 2), but using the alternative weight function depicted in Fig. 3. Its main characteristic is that the influence of the actual point is removed, and the highest weight is located at a distance of  $0.707l_s$ , where  $l_s$  controls the width of the symmetrical curves, acting as the internal length scale.

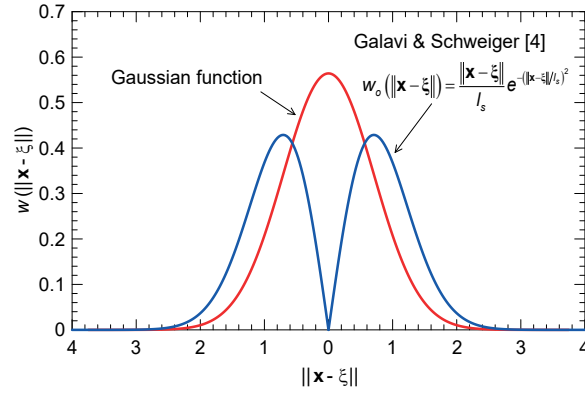


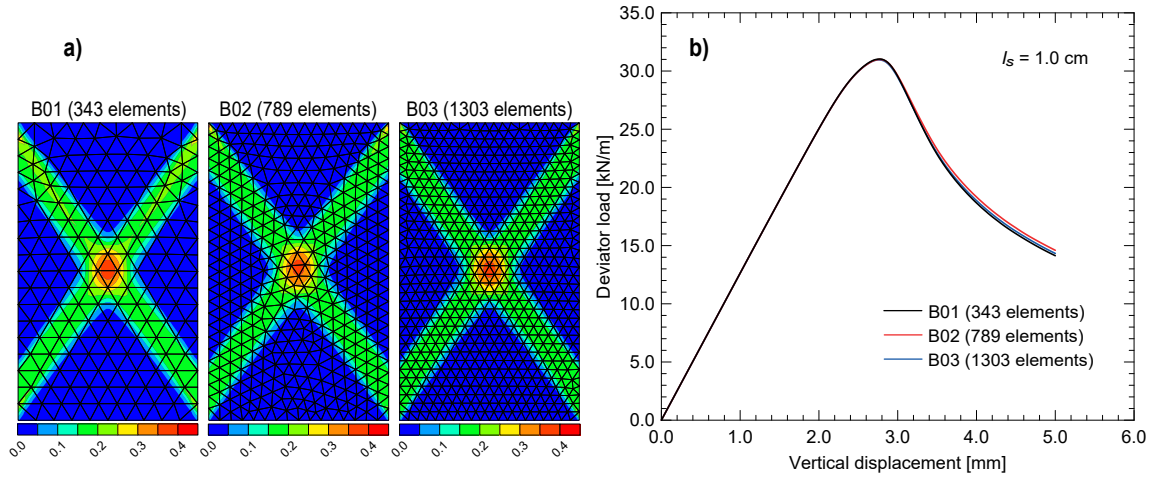
**Figure 3:** Representation of the weight function from [4]

In the implementation of this approach, the nonlocal state variable is computed only for points in the softening regime, and considering neighbouring points at distances lower than  $2l_s$  [4].

### 3 STRAIN LOCALIZATION ANALYSES

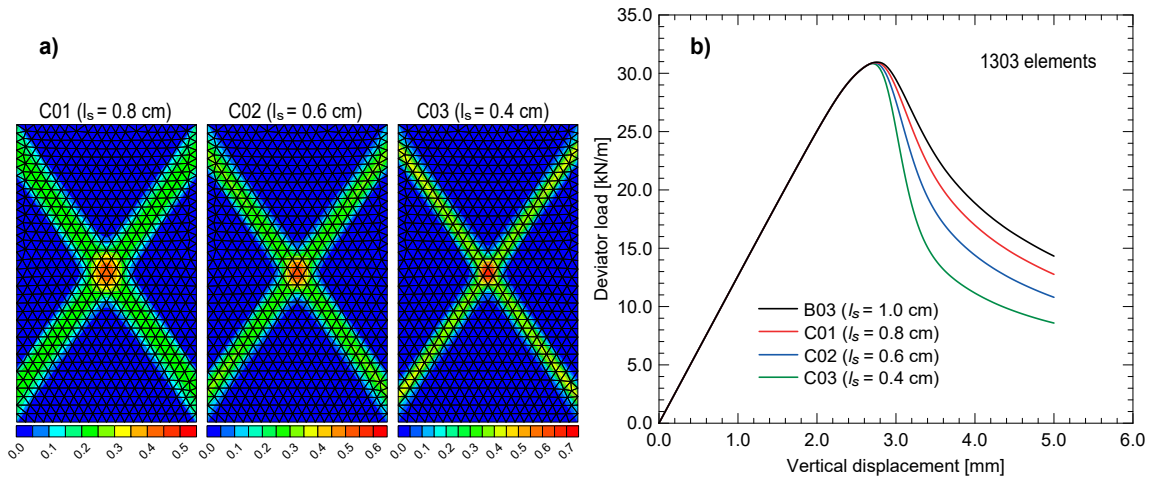
A number of two-dimensional analyses were performed to assess the developed constitutive model for the simulation of localized deformation patterns, corresponding to a drained biaxial plane strain test under displacement control. The specimen is 6 cm width and 10 cm height and fixed horizontal displacement were considered at the top and bottom ends, in order to develop a non-homogeneous stress/strain field and favour the onset of localization.

Fig. 4a shows the contours of shear strain ( $\epsilon_s = (\epsilon_1 - \epsilon_3)/2$ ) of three analyses with different meshes and  $l_s = 1.0$  cm. Because of the rough boundary conditions, stresses concentrate at the four corners of the model, allowing the simultaneous formation of two X-shaped shear bands. In the three analyses, the same localization pattern and the same width of shear bands were obtained regardless the number of elements. In addition, an almost unique force-displacement curve was obtained (Fig. 4b), demonstrating the ability of the approach to deliver objective results.



**Figure 4:** (a) Contours of shear strain and (b) force-displacement curves for different meshes

The effect of  $l_s$  on the configuration of shear bands is shown in Fig. 5a. As  $l_s$  is decreased, the interaction zone (considered neighbouring Gauss points) is also decreased, and plastic deformations tend to localize in a narrower zone. The width of the numerical shear bands is roughly equal to  $l_s$ , as already obtained by [4]. However, a thinner shear band renders a lower energy dissipation, and therefore a more brittle response (Fig. 5b). In the simulation of a given material, the constitutive softening rate can be adjusted to match the desired global force-displacement response for a given  $l_s$ ; a technique known as *softening scaling* [4].



**Figure 5:** (a) Contours of shear strain and (b) force-displacement curves for different length scale parameters

The onset of localization was identified by the evolution of the second derivative of the shear strain with respect to time, averaged from all Gauss points ( $\bar{\epsilon}_s''$ ), i.e. some sort of global shear strain acceleration. Fig. 6a shows the evolution of this variable during

one of the analysis. A distinct jump is clearly identified, suggested here as the onset of localization of the BVP. This point does not necessarily occurs at the global peak strength, and in this case occurs slightly before it. Its actual location seems to be controlled by the amount of points entering to the softening regime before the peak strength, which in turn is mainly the result of the considered boundary conditions.

Regarding the orientation of shear bands, this problem has been historically bounded by two limits: the upper bound given by Coulomb's theory ( $\theta_C = 45^\circ + \phi/2$ ), and the lower bound given by Roscoe's solution [5] ( $\theta_R = 45^\circ + \psi/2$ ) ( $\phi$  and  $\psi$  are the mobilized friction and dilation angles). The theoretical orientation given by these solutions has been computed in one of the analyses, at a point within the shear band, and the results have been compared to the actual inclination obtained from the simulation (Fig. 6b). Coulomb's orientation seems to overestimate the obtained shear band inclination, which appears to coincide with Roscoe's solution at the onset of localization.

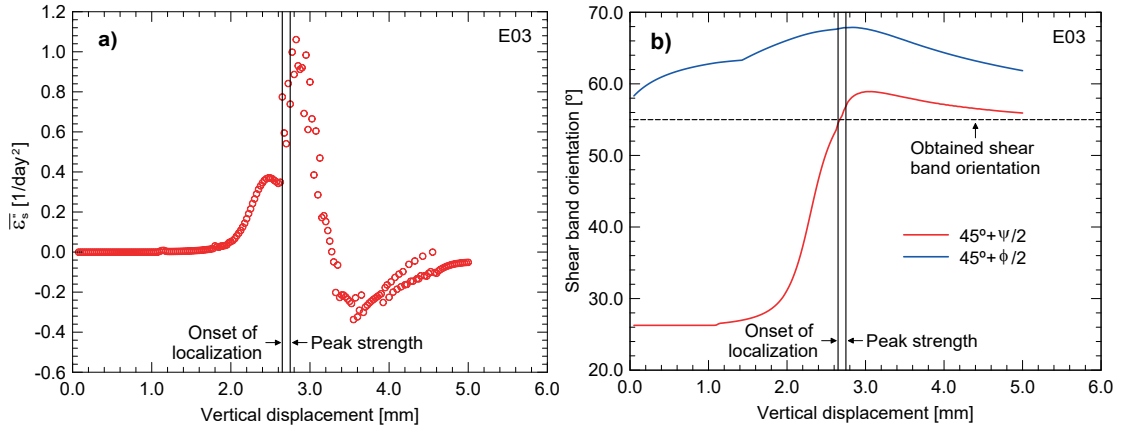


**Figure 6:** (a) Onset of localization and (b) theoretical and obtained shear band orientations

Since the amount of dilation at the onset of localization seems to control the orientation of the shear band, a given BVP should render a different orientation if the flow rule (Eq. 3) of the constitutive law is modified. The latter is shown in Fig. 7, where the same analysis was performed using different values of  $\omega$ , controlling the amount of volumetric plastic strains (vertical displacements were normalized with the corresponding value at the onset of localization). As  $\omega$  is reduced, a smaller  $\psi$  is attained at the onset of localization, rendering a gentler inclination of shear bands. Nevertheless, the obtained orientations can again be explained in terms of Roscoe's solution at the onset of localization.

## 4 CONCLUSIONS

A nonlocal plasticity model has been described, aimed to reproduce the strength characteristics of stiff fine-grained soils, including the objective simulation of strain localization. The selected results presented here, provide useful insights into relevant aspects of the numerical simulation of strain localization, and demonstrate the capability of the approach to simulate localized deformation patterns.

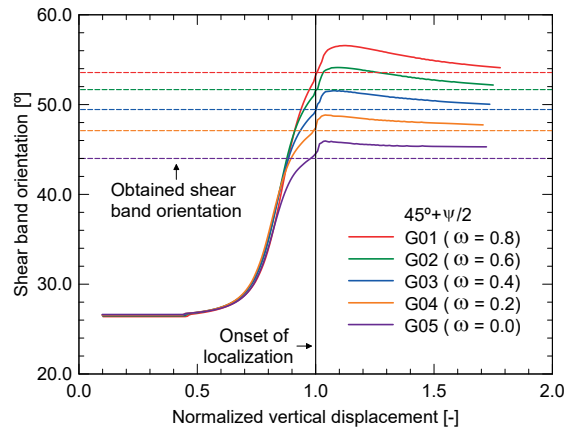


**Figure 7:** Theoretical and obtained shear band orientations for different flow rules

## REFERENCES

- [1] A. Gens, “On the hydromechanical behaviour of argillaceous hard soils-weak rocks (Keynote Lecture),” in *Geotechnics of Hard Soils Weak Rocks, Proceedings of the 15th European Conference on Soil Mechanics and Geotechnical Engineering*, vol. 4, (London), pp. 71–118, Thomas Telford, 2011.
- [2] R. J. Jardine, A. Gens, D. W. Hight, and M. R. Coop, “Developments in understanding soil behaviour,” in *Advances in geotechnical engineering: The Skempton conference* (R. J. Jardine, D. M. Potts, and K. G. Higgins, eds.), pp. 103–206, 2004.
- [3] Z. P. Bažant and M. Jirásek, “Nonlocal Integral Formulations of Plasticity and Damage: Survey of Progress,” *Journal of Engineering Mechanics*, vol. 128, no. 11, pp. 1119–1149, 2002.
- [4] V. Galavi and H. F. Schweiger, “Nonlocal Multilaminate Model for Strain Softening Analysis,” *International Journal of Geomechanics*, vol. 10, no. 1, pp. 30–44, 2010.
- [5] K. H. Roscoe, “The influence of strains in soil mechanics,” *Géotechnique*, vol. 20, no. 2, pp. 129–170, 1970.